

The antiapoptotic protein Bcl-xL negatively regulates the bone-resorbing activity of osteoclasts in mice

Mitsuyasu Iwasawa,¹ Tsuyoshi Miyazaki,² Yuichi Nagase,¹ Toru Akiyama,¹ Yuho Kadono,¹ Masaki Nakamura,¹ Yasushi Oshima,¹ Tetsuro Yasui,¹ Takumi Matsumoto,¹ Takashi Nakamura,³ Shigeaki Kato,³ Lothar Hennighausen,⁴ Kozo Nakamura,¹ and Sakae Tanaka¹

¹Department of Orthopaedic Surgery, Faculty of Medicine, University of Tokyo, Tokyo, Japan. ²Department of Geriatric Medicine, Tokyo Metropolitan Geriatric Hospital and Institute of Gerontology, Tokyo, Japan. ³Institute of Molecular and Cellular Biosciences, University of Tokyo, Tokyo, Japan. ⁴Laboratory of Genetics and Physiology, NIH, Bethesda, Maryland, USA.

The B cell lymphoma 2 (Bcl-2) family member Bcl-xL has a well-characterized antiapoptotic function in lymphoid cells. However, its functions in other cells – including osteoclasts, which are of hematopoietic origin – and other cellular processes remain unknown. Here we report an unexpected function of Bcl-xL in attenuating the bone-resorbing activity of osteoclasts in mice. To investigate the role of Bcl-xL in osteoclasts, we generated mice with osteoclast-specific conditional deletion of *Bcl-x* (referred to herein as *Bcl-x* cKO mice) by mating *Bcl-x*^{fl/fl} mice with mice in which the gene encoding the Cre recombinase has been knocked into the *cathepsin K* locus and specifically expressed in mature osteoclasts. Although the *Bcl-x* cKO mice grew normally with no apparent morphological abnormalities, they developed substantial osteopenia at 1 year of age, which was caused by increased bone resorption. *Bcl-x* deficiency increased the bone-resorbing activity of osteoclasts despite their high susceptibility to apoptosis, whereas Bcl-xL overexpression produced the opposite effect. In addition, *Bcl-x* cKO osteoclasts displayed increased c-Src activity, which was linked to increased levels of vitronectin and fibronectin expression. These results suggest that Bcl-xL attenuates osteoclastic bone-resorbing activity through the decreased production of ECM proteins, such as vitronectin and fibronectin, and thus provide evidence for what we believe to be a novel cellular function of Bcl-xL.

Introduction

Osteoclasts are highly differentiated bone-resorbing cells of hematopoietic origin. Bone resorption is a multistep process: the initial attachment of osteoclasts to bone matrix leads to cytoskeletal reorganization, cellular polarization, and formation of unique membrane areas for bone resorption (1, 2). During resorption, osteoclasts develop a specific ring structure of microfilaments called the sealing zone, which mediates tight attachment of the cells to mineralized bone matrix (3, 4). Although these bone resorption processes are composed of multiple but highly regulated steps, the molecular basis governing these processes is barely understood.

B cell lymphoma 2 (Bcl-2) family member proteins consist of more than 30 proteins, including anti- and proapoptotic proteins that share up to 4 conserved regions known as the Bcl-2 homology (BH) domains (5). Antiapoptotic Bcl-2 family members, such as Bcl-2 and Bcl-xL, contain all 4 BH domain subtypes and promote cell survival by inhibiting the function of the proapoptotic Bcl-2 proteins. Anti- and proapoptotic Bcl-2 proteins can be found in the cytosol, endoplasmic reticulum, mitochondria, and nuclear envelope (6–9). Antiapoptotic Bcl-2 family members also inhibit proapoptotic Bax and Bak from inducing permeabilization of the outer mitochondrial membrane and the subsequent release of apoptogenic molecules, such as cytochrome *c* and SMAC/DIABLO, which leads to caspase activation. However, the role of Bcl-2 family members in the other cellular events remains to be characterized.

Bcl-xL, originally identified from chicken lymphoid cells as an antiapoptotic protein belonging to the Bcl-2 family, is a major isoform produced by alternative splicing of the *bcl-x* gene (10). The role of Bcl-xL in osteoclasts has not been elucidated yet, and conventional *Bcl-x*-null mice – because of increased apoptosis of postmitotic immature neurons and hematopoietic cells of the liver – are embryonically lethal by day 13 (11), which severely hampers the analysis of their osteoclasts. Here, we report the unexpected finding that Bcl-xL regulated not only the survival of osteoclasts, but also their bone-resorbing activity, both in vitro and in vivo. Osteoclast-specific *Bcl-x*-null mice exhibited reduced bone mass caused by increased bone-resorbing function of osteoclasts. c-Src kinase activity increased in *Bcl-x*-deficient osteoclasts by means of increased expression levels of ECM proteins, such as vitronectin and fibronectin. These observations point to what we believe to be a novel link between Bcl-xL and the bone-resorbing activity of mature osteoclasts.

Results

The Bcl-2/Bcl-xL inhibitor ABT-737 suppressed survival, but increased bone-resorbing activity, of osteoclasts. To determine whether antiapoptotic Bcl-2 family proteins affect the survival and bone-resorbing activity of mature osteoclasts, we first examined the effect of ABT-737, a small-molecule BH3 mimetic that binds to and antagonizes Bcl-2 and Bcl-xL, but not Mcl-1 (12), on osteoclasts. As expected, treatment with 10 μM ABT-737 severely diminished osteoclast survival (Figure 1A). Interestingly, ABT-737 treatment upregulated the bone-resorbing activity of osteoclasts (Figure 1B), which suggests that antiapoptotic Bcl-2 family pro-

Conflict of interest: The authors have declared that no conflict of interest exists.

Citation for this article: *J. Clin. Invest.* 119:3149–3159 (2009). doi:10.1172/JCI39819.

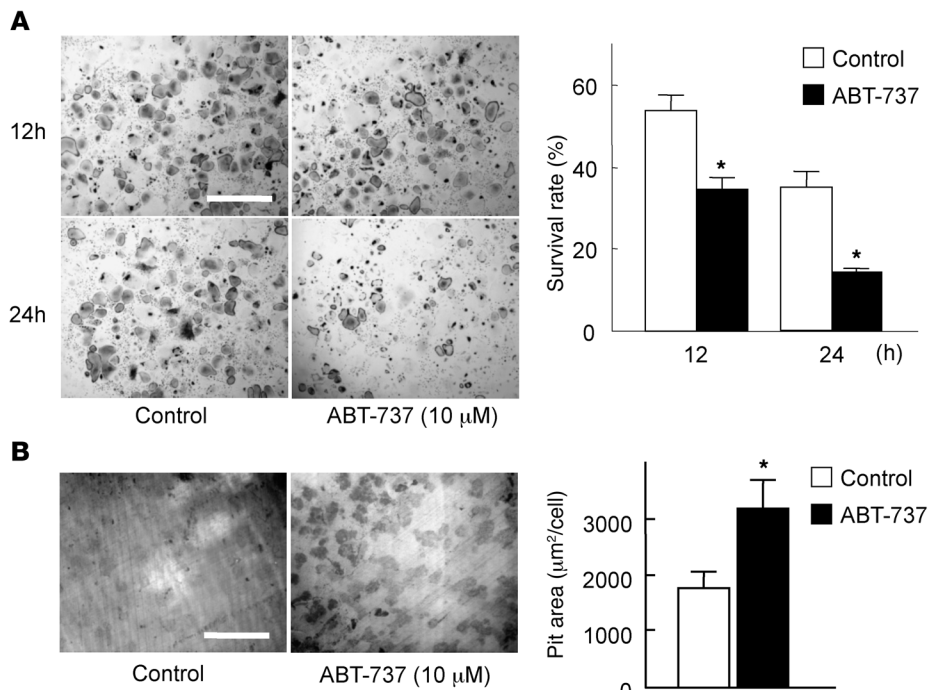


Figure 1 The Bcl-2/Bcl-xL inhibitor ABT-737 suppressed survival, but enhanced the bone-resorbing activity, of osteoclasts. **(A)** For survival assay, we used bone marrow–derived osteoclasts generated on regular dishes in the presence of 100 ng/ml RANKL and 10 ng/ml M-CSF. On day 5 of culture (time 0), when osteoclasts were differentiated, they were further cultured with or without 10 μM ABT-737 and subjected to TRAP staining. The number of viable cells after 12 or 24 hours of ABT-737 treatment is shown as a percentage of morphologically intact osteoclasts compared with time 0. TRAP staining of representative cultures is also shown. **(B)** For pit formation assay, osteoclasts were generated by cocultures of osteoblasts and bone marrow cells on collagen gel–coated dishes in the presence of 10 nM 1 α ,25(OH)₂vitamin D₃ and 1 μM PGE₂. On day 6 of culture, when osteoclasts were differentiated, cells were dispersed by treating with 0.1% collagenase for 10 minutes, resuspended in α -MEM containing 10% FBS, and replated on dentine slices in the presence or absence of 10 μM ABT-737. After 24 hours of culture, cells were removed by treating the dentine slices with 1M NH₄OH, and pit area was visualized by toluidine blue staining and quantified by image analysis system. Resorption pits of representative cultures are also shown. **(A and B)** Results are mean \pm SD of 6 cultures. **P* < 0.01 versus untreated control. Scale bars: 500 μm.

teins negatively regulate osteoclastic bone resorption in spite of their positive effect on osteoclast survival.

Osteoclast-specific bcl-x knockout mice exhibit decreased bone mass through increased osteoclastic bone resorption. To investigate the role of Bcl-xL in osteoclasts in further detail, we generated osteoclast-specific *Bcl-x* conditional knockout (cKO) mice by mating *Bcl-x^{fl/fl}* mice with cathepsin K-Cre transgenic mice, in which the Cre recombinase gene is inserted into the *cathepsin K* locus and specifically expressed in osteoclasts (13). The resulting cathepsin K-Cre^{+/+}-*Bcl-x^{fl/fl}* mice (referred to herein as *Bcl-x* cKO mice) were born alive at predicted Mendelian frequencies. Bcl-xL was markedly reduced in osteoclasts from *Bcl-x* cKO mice, while its expression in osteoblasts (Figure 2A) and other tissues (data not shown) in *Bcl-x* cKO mice was comparable to that found in normal cathepsin K-Cre^{-/-}-*Bcl-x^{fl/fl}* littermates (Figure 2A).

Although *Bcl-x* cKO mice grew normally with no apparent morphological abnormalities, 8-week-old *Bcl-x* cKO mice exhibited a decrease in trabecular bone volume by histological and histomorphometric analysis (Figure 2, B and C), and the mice

developed substantial osteopenia at 1 year of age, as determined by radiological analyses (Figure 3, A and B). Histomorphometric analysis of 8-week-old *Bcl-x* cKO mice revealed a significant increase in the eroded surface/bone surface ratio, but not in osteoclast number or osteoclast surface, and the bone formation parameters were equivalent to those in normal *Bcl-x^{fl/fl}* littermates (Figure 2B). Bone mineral density of the distal femur of 1-year-old *Bcl-x* cKO mice was significantly lower than that of normal *Bcl-x^{fl/fl}* littermates (Figure 3C), and μ CT analysis revealed significant decreases in bone volume per tissue volume, trabecular thickness, and trabecular bone number – and a significant increase in trabecular separation – in *Bcl-x* cKO mice compared with normal *Bcl-x^{fl/fl}* littermates (Figure 3B). In addition, levels of serum C-terminal cross-linking telopeptide of type 1 collagen (CTX-1), a marker of bone resorption, significantly increased in 1-year-old *Bcl-x* cKO mice compared with those of normal *Bcl-x^{fl/fl}* littermates (Figure 3D). Collectively, these findings suggest that bone loss in the *Bcl-x* cKO mouse is caused by increased bone-resorbing activity of mature osteoclasts, rather than by decreased bone formation.

Bcl-xL regulates the survival of osteoclasts. To further confirm the role of Bcl-xL in osteoclast survival, we used an adenovirus vector–mediated gene transduction system. In the absence of trophic factors such as M-CSF, approximately 40% and 80% of noninfected osteoclasts (data not shown) and osteoclasts (Figure 4A) infected with adenovirus vector carrying GFP (AxGFP) died within 12 and 24 hours, respectively. Overexpression of Bcl-xL remarkably enhanced the survival of osteoclasts (Figure 4A) and decreased the expression level of cleaved caspase-3, a primary executioner caspase inducing apoptosis (Figure 4B). We then obtained *Bcl-x^{fl/fl}* osteoclasts by adenoviral introduction of Cre recombinase into the osteoclasts generated from bone marrow cells of *Bcl-x^{fl/fl}* mice. *Bcl-x^{fl/fl}* osteoclasts generated by infection with adenovirus vector carrying Cre recombinase (AxCre) displayed high Cre expression and decreased Bcl-xL expression (Figure 4C) and exhibited reduced survival associated with the increased expression of cleaved caspase-3 (Figure 4, D and E). We next generated *Bcl-x* cKO osteoclasts by treating bone marrow cells from *Bcl-x* cKO mice with RANKL and M-CSF. As shown in Figure 4F, *Bcl-x* cKO osteoclasts exhibited reduced survival compared with *Bcl-x^{fl/fl}* osteoclasts, which was completely rescued by adenovirus-mediated overexpression of Bcl-xL.

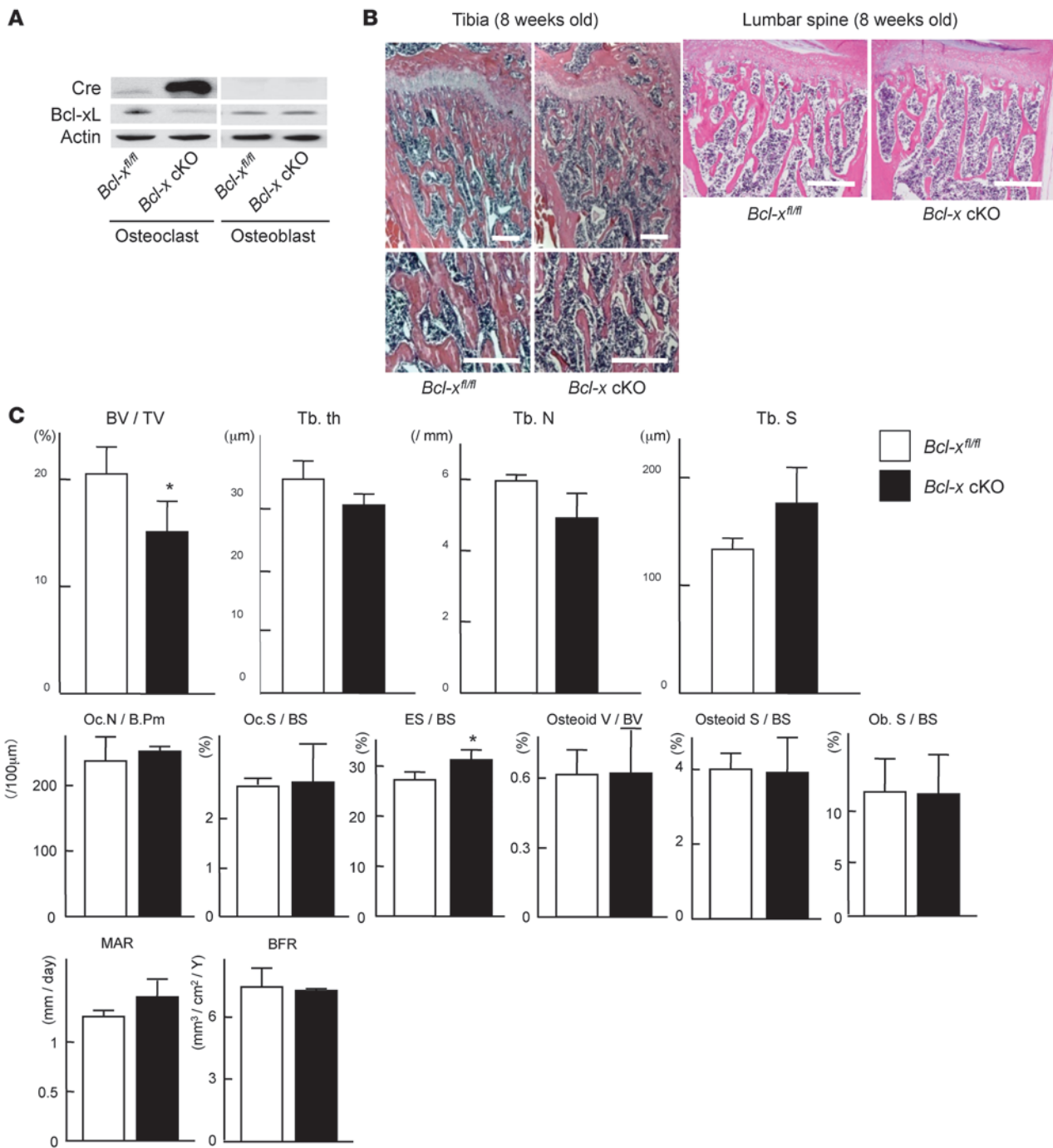


Figure 2

Generation and skeletal analysis of *Bcl-x* cKO mice. **(A)** Western blotting of Cre recombinase and Bcl-xL in *Bcl-x* cKO mice and their normal *Bcl-x^{fl/fl}* littermates using β-actin as an internal control. Bcl-xL expression was markedly reduced in osteoclasts, but not in osteoblasts, of *Bcl-x* cKO mice. **(B)** Histological sections of proximal tibia and lumbar spine of male *Bcl-x* cKO mice and their normal *Bcl-x^{fl/fl}* littermates at 8 weeks of age. *Bcl-x* cKO mice exhibited reduced bone mass. Scale bars: 100 μm. **(C)** Histomorphometric analysis of male *Bcl-x* cKO mice and their normal *Bcl-x^{fl/fl}* littermates at 8 weeks of age. Bone volume per trabecular volume (BV/TV) significantly decreased in *Bcl-x* cKO mice ($P < 0.01$). Trabecular bone thickness (Tb.th) and trabecular bone number (Tb.N) was reduced, and the trabecular separation (Tb.S) was increased, in *Bcl-x* cKO mice, with marginal statistical difference ($P < 0.1$). As for osteoclast markers, whereas the eroded surface/bone surface (ES/BS) significantly increased in *Bcl-x* cKO mice ($P < 0.05$), neither osteoclast number nor osteoclast surface increased. The parameters of bone formation in *Bcl-x* cKO mice were equivalent to those of normal littermates. Results are mean ± SD of 3 different samples. * $P < 0.01$ versus normal *Bcl-x^{fl/fl}* littermates. Oc.N/B.Pm, number of mature osteoclasts per 100-μm bone perimeter; Oc.S/BS, bone surface covered by mature osteoclasts; Osteoid V/BV, osteoid volume per bone volume; Osteoid S/BS, osteoid surface per bone surface; Ob.S/BS, bone surface covered by cuboidal osteoblasts; MAR, mineral apposition rate; BFR, bone formation rate.

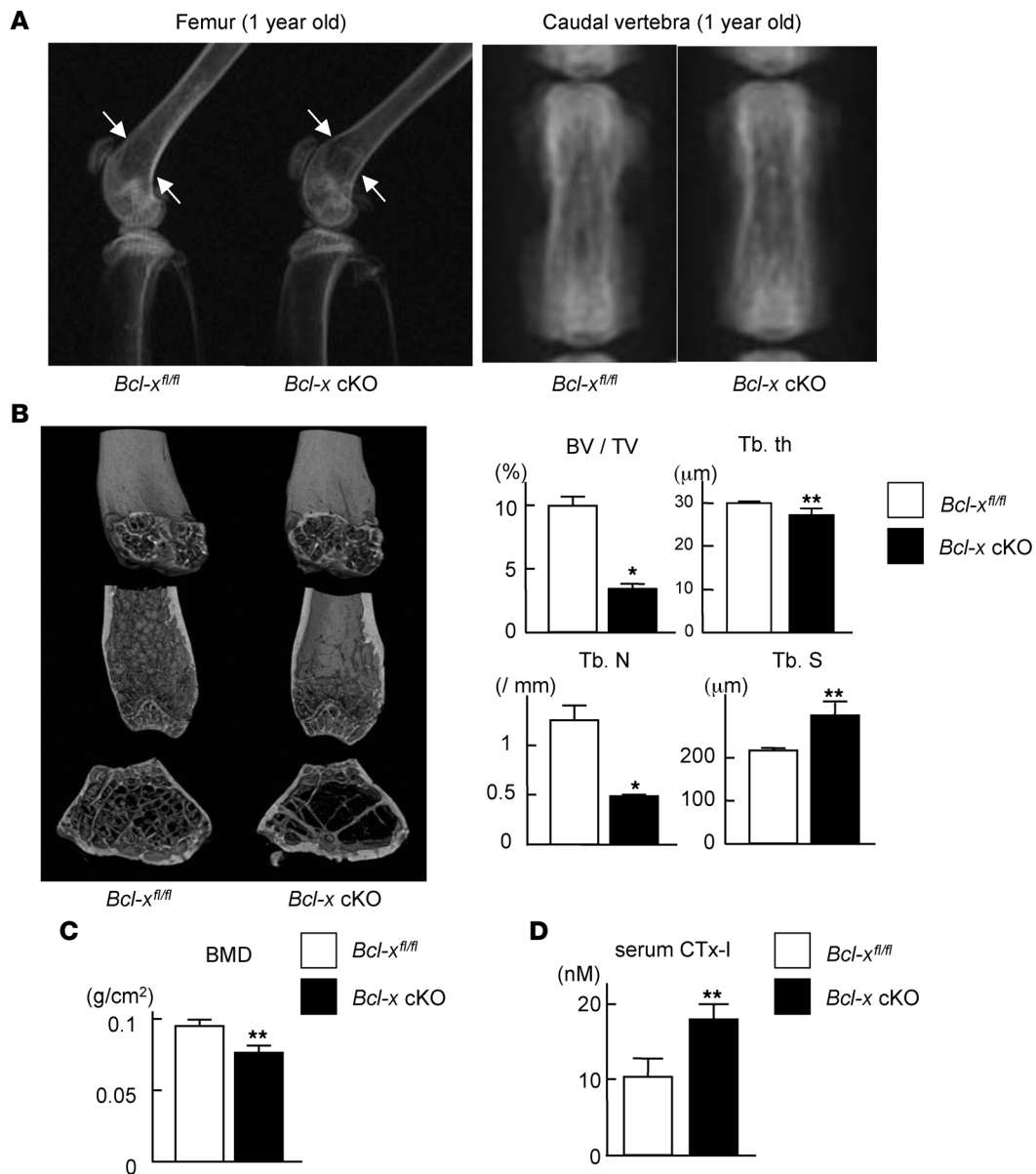


Figure 3

Generation and skeletal analysis of *Bcl-x* cKO mice. **(A)** Representative radiography images of the lower extremities and caudal vertebra of male *Bcl-x* cKO mice and their normal *Bcl-x^{fl/fl}* littermates at 1 year of age. *Bcl-x* cKO mice exhibited reduced bone mass (arrows). **(B)** Distal femur μ CT in male *Bcl-x* cKO mice and their normal *Bcl-x^{fl/fl}* littermates at 1 year of age. Bone volume per trabecular volume and trabecular bone number were significantly reduced, and trabecular separation was significantly increased, in *Bcl-x* cKO mice. **(C)** Bone mineral density (BMD) of the distal femur was significantly reduced in male *Bcl-x* cKO mice at 1 year of age compared with normal *Bcl-x^{fl/fl}* littermates. **(D)** Serum concentration of CTx-I significantly increased in 1-year-old *Bcl-x* cKO mice. **(B–D)** Results are mean \pm SD of 3 different samples. * $P < 0.01$, ** $P < 0.05$ versus normal *Bcl-x^{fl/fl}* littermates.

Bcl-xL mediates prosurvival activity downstream of Erk in osteoclasts. We previously reported that Erk activation markedly promotes osteoclast survival (14). Therefore, we sought to determine the effect of the relationship between Erk and *Bcl-xL* on osteoclast survival. First, we examined whether *Bcl-xL* expression affects Erk activity in osteoclasts. *Bcl-xL* overexpression suppressed Erk activity in osteoclasts, while knockout of *Bcl-x* by overexpression of Cre recombinase in *Bcl-x^{fl/fl}* osteoclasts increased it (Figure 5A), suggesting negative feedback regulation of Erk activity by *Bcl-xL*. We

further examined whether Erk activity affects *Bcl-xL* expression in osteoclasts. Activation of Erk pathways by adenovirus-mediated overexpression of constitutively active Mek1 (Mek^{CA}) increased *Bcl-xL* expression in osteoclasts. Furthermore, suppression of the pathways by introduction of dominant-negative Ras (Ras^{DN}) decreased *Bcl-xL* expression in osteoclasts (Figure 5A). In addition, reduced osteoclast survival by Ras^{DN} overexpression (Figure 5B) or treatment with the Mek inhibitor PD98059 (Figure 5C) was completely rescued by *Bcl-xL* overexpression, while *Bcl-x* deficiency

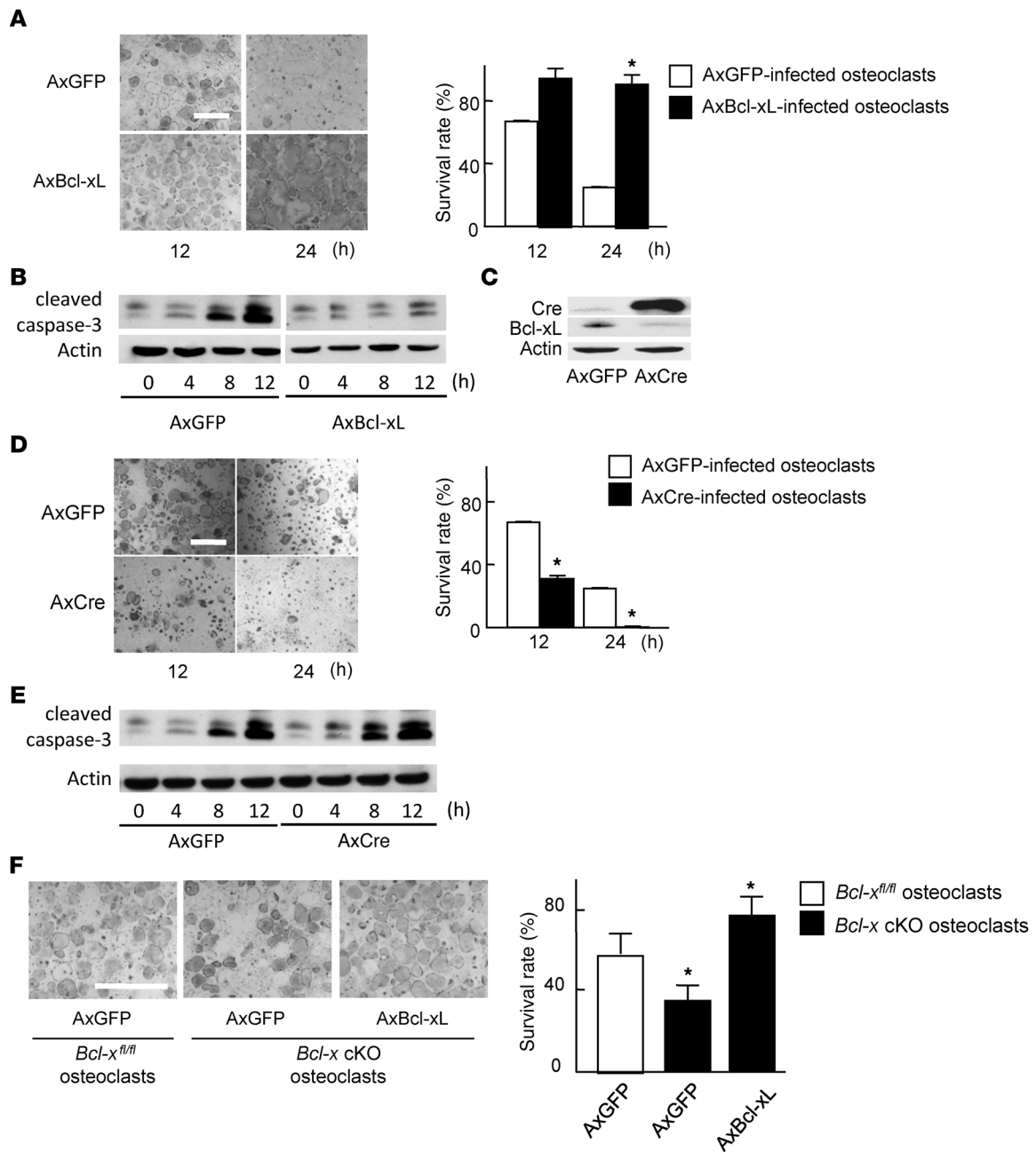


Figure 4

Bcl-xL regulates osteoclast survival. (A) Adenovirus-mediated overexpression of Bcl-xL markedly suppressed cell death of wild-type osteoclasts. TRAP staining of representative cultures is also shown. (B) Western blotting of cleaved caspase-3 using β -actin as an internal control. Bcl-xL overexpression suppressed the amount of cleaved caspase-3 in osteoclasts. Lanes from this panel were run on the same gel but were noncontiguous. (C) Adenovirus vector-mediated overexpression of Cre recombinase efficiently downregulated Bcl-xL expression in osteoclasts differentiated from *Bcl-x*^{fl/fl} mouse bone marrow cells. (D) Increased cell death in *Bcl-x* cKO osteoclasts. TRAP staining of representative cultures is also shown. (E) Western blotting of cleaved caspase-3 using β -actin as an internal control. *Bcl-x* cKO osteoclasts exhibited the amount of increased cleaved caspase-3. (F) Decreased survival in *Bcl-x* cKO osteoclasts was rescued by Bcl-xL overexpression. Osteoclasts were generated from bone marrow cells of *Bcl-x* cKO mice or their normal *Bcl-x*^{fl/fl} littermates, infected with either AxGFP or AxBcl-xL, and subjected to survival assay. After 24 h of culture, osteoclasts derived from *Bcl-x* cKO mouse bone marrow cells exhibited reduced survival, which was rescued by Bcl-xL introduction. (A, D, and F) Results are mean \pm SD. **P* < 0.01 versus AxGFP-infected control. Scale bars: 500 μ m.

reduced the prosurvival effect of Mek^{CA} (Figure 5D). These results suggest that the prosurvival effect of Erk activation is mediated, at least in part, by the induction of Bcl-xL expression, and that Bcl-xL in turn negatively regulates Erk activity.

Bcl-xL deficiency stimulates bone resorption by upregulating *c-Src* activity. We next investigated the role of Bcl-xL in the bone-resorbing activity of osteoclasts. As shown in Figure 6, A and B, the bone-resorbing activity of osteoclasts overexpressing *Bcl-xL* signifi-

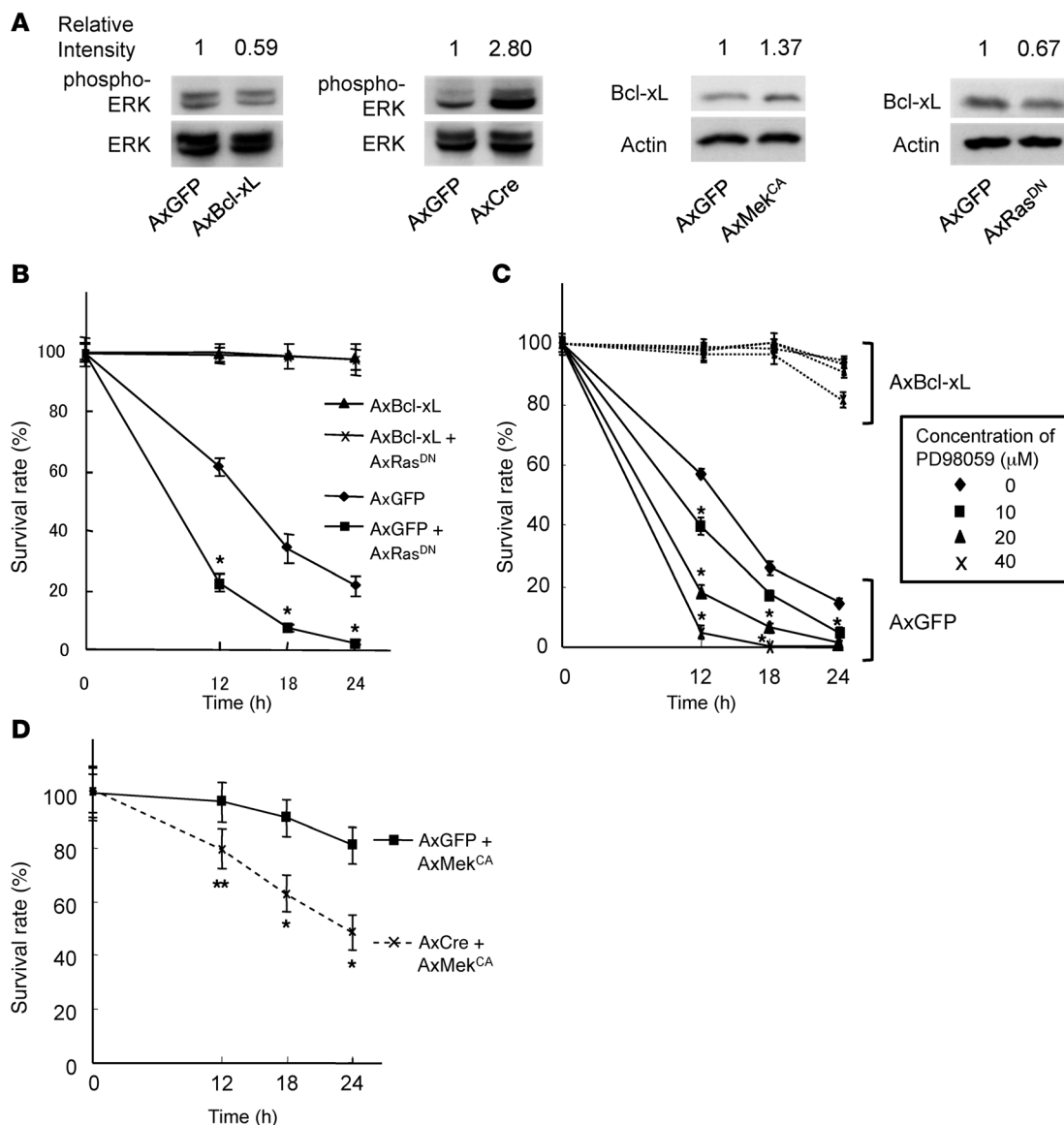


Figure 5

Ras-Mek-Erk pathways are upstream of Bcl-xL in osteoclasts. (A) *Bcl-x^{fl/fl}* osteoclasts were infected with AxGFP, AxCre, AxBcl-xL, AxMek^{CA}, or AxRas^{DN}. Bcl-xL overexpression by AxBcl-xL infection suppressed, and knockout of *Bcl-x* gene by AxCre infection increased, Erk activity, as determined by the amount of phospho-Erk in *Bcl-x^{fl/fl}* osteoclasts. In contrast, AxMek^{CA} infection increased, and AxRas^{DN} infection decreased, Bcl-xL expression. Relative intensity of the bands on each gel, measured by densitometry, is shown above each lane. (B) *Bcl-x^{fl/fl}* osteoclasts were infected with AxGFP, AxGFP plus AxRas^{DN}, AxBcl-xL, or AxBcl-xL plus AxRas^{DN}. Reduced osteoclast survival by Ras^{DN} overexpression was completely rescued by Bcl-xL overexpression. **P* < 0.01 versus AxGFP-infected cells. (C) *Bcl-x^{fl/fl}* osteoclasts were infected with AxGFP or AxBcl-xL, and then treated with the indicated concentrations of MEK inhibitor PD98059. PD98059 treatment dose-dependently suppressed the survival of osteoclasts, which was completely rescued by Bcl-xL overexpression. **P* < 0.01 versus untreated osteoclasts. (D) *Bcl-x^{fl/fl}* osteoclasts were infected with AxGFP or AxCre together with AxMek^{CA}. Prosurvival effect of Mek^{CA} overexpression was partially suppressed by *Bcl-x* deletion. **P* < 0.01, ***P* < 0.05 versus AxGFP-AxMek^{CA}-infected cells. All results are mean \pm SD of 6 cultures.

cantly decreased, and that of *Bcl-x*-deficient osteoclasts significantly increased, compared with AxGFP-infected osteoclasts. In addition, *Bcl-x* cKO osteoclasts also exhibited an increase in bone resorption, which was suppressed by Bcl-xL overexpression (Figure 6C). These results indicate a negative regulatory role of Bcl-xL in osteoclastic bone resorption.

Because c-Src is known to be a critical regulator of osteoclast function (15, 16), we examined whether the expression level of

Bcl-xL affects c-Src activity in osteoclasts. As assessed by Western blotting, the phosphorylation level of c-Src at activating tyrosine residue (Y416) was modulated in a manner opposite to the expression level of Bcl-xL, while the phosphorylation activity of Akt remained unchanged by Bcl-xL expression level (Figure 7A). These results suggest that the upregulation of *Bcl-x* cKO osteoclasts' bone-resorbing activity is promoted, at least in part, by c-Src activation.

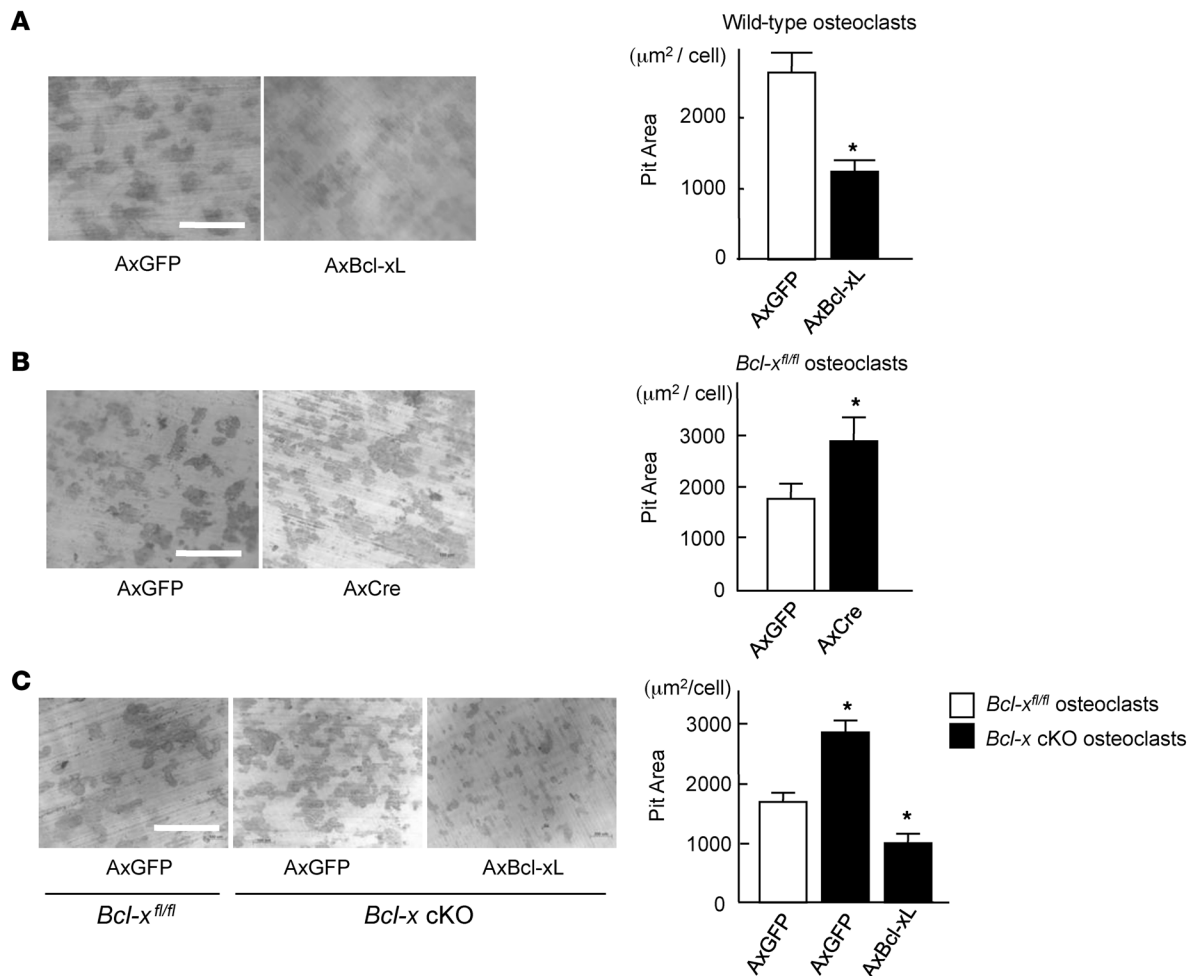


Figure 6 Effect of Bcl-xL on bone-resorbing activity of osteoclasts. (A) Adenovirus vector-mediated Bcl-xL overexpression suppressed pit formation by osteoclasts. Osteoclasts generated from normal mice were infected with AxGFP or AxBcl-xL, and then subjected to pit formation assay. Representative resorption pits, visualized by toluidine blue staining, are also shown. Results are mean ± SD of 6 cultures. (B) Osteoclasts generated from *Bcl-x^{fl/fl}* mouse bone marrow cells were infected with AxGFP or AxCre and subjected to pit formation assay. *Bcl-x* deficiency increased bone resorption by osteoclasts. Representative resorption pits, visualized by toluidine blue staining, are also shown. Results are mean ± SD of 6 cultures. (C) Osteoclasts were generated from bone marrow cells of *Bcl-x* cKO mice or their normal *Bcl-x^{fl/fl}* littermates, infected with AxGFP or AxBcl-xL, and subjected to pit formation assay. *Bcl-x* cKO osteoclasts exhibited increased bone-resorbing activity, which was suppressed by Bcl-xL introduction. Representative resorption pits, visualized by toluidine blue staining, are also shown. Experiments were repeated 3 times using different mice, and results are mean ± SD. (A–C) **P* < 0.01 versus AxGFP-infected osteoclasts. Scale bars: 500 µm.

Bcl-xL regulates the expression of ECM proteins in osteoclasts. We ultimately examined how c-Src kinase activity is regulated by Bcl-xL in osteoclasts. In many cell types, cell attachment to the ECM through integrins leads to the activation of several protein tyrosine kinases and the formation of focal adhesions, multiprotein complexes that anchor actin stress fibers to the cytoplasmic face of the plasma membrane (17). Both $\alpha_v\beta_3$ integrins, the predominant integrin expressed in osteoclasts, and c-Src have been reported to play crucial roles in the cell migration and bone-resorbing activity of osteoclasts (15, 18). Because the levels of the β_3 subunits in osteoclasts remained unchanged by *Bcl-x* disruption (data not shown), we examined the expression of ECM proteins. *Bcl-x* disruption by AxCre infection upregulated the expression levels of vitronectin and fibronectin, but not osteopontin, in osteoclasts generated from *Bcl-x^{fl/fl}* mouse bone marrow cells; conversely, Bcl-xL overex-

pression displayed the opposite effect (Figure 7B). We then inoculated osteoclasts infected with adenovirus vector carrying Bcl-xL (AxBcl-xL) onto uncoated dentine slices or dentine slices coated with vitronectin or fibronectin and cultured them for 12 hours. Similar to our findings described above, osteoclasts overexpressing Bcl-xL exhibited reduced bone-resorbing activity on uncoated dentine slices. However, when they were cultured on vitronectin- or fibronectin-coated dentine slices, the negative effect of Bcl-xL overexpression on bone resorption was partially reversed, and a significant increase in pit area was observed when they were cultured on vitronectin-coated dentine slices (*P* < 0.05; Figure 7C). Reduced c-Src activity was also restored by plating the cells on vitronectin- or fibronectin-coated dishes (Figure 7D). Taken together, these results indicate that the regulation of ECM proteins by Bcl-xL is an important component of osteoclastic bone resorption.

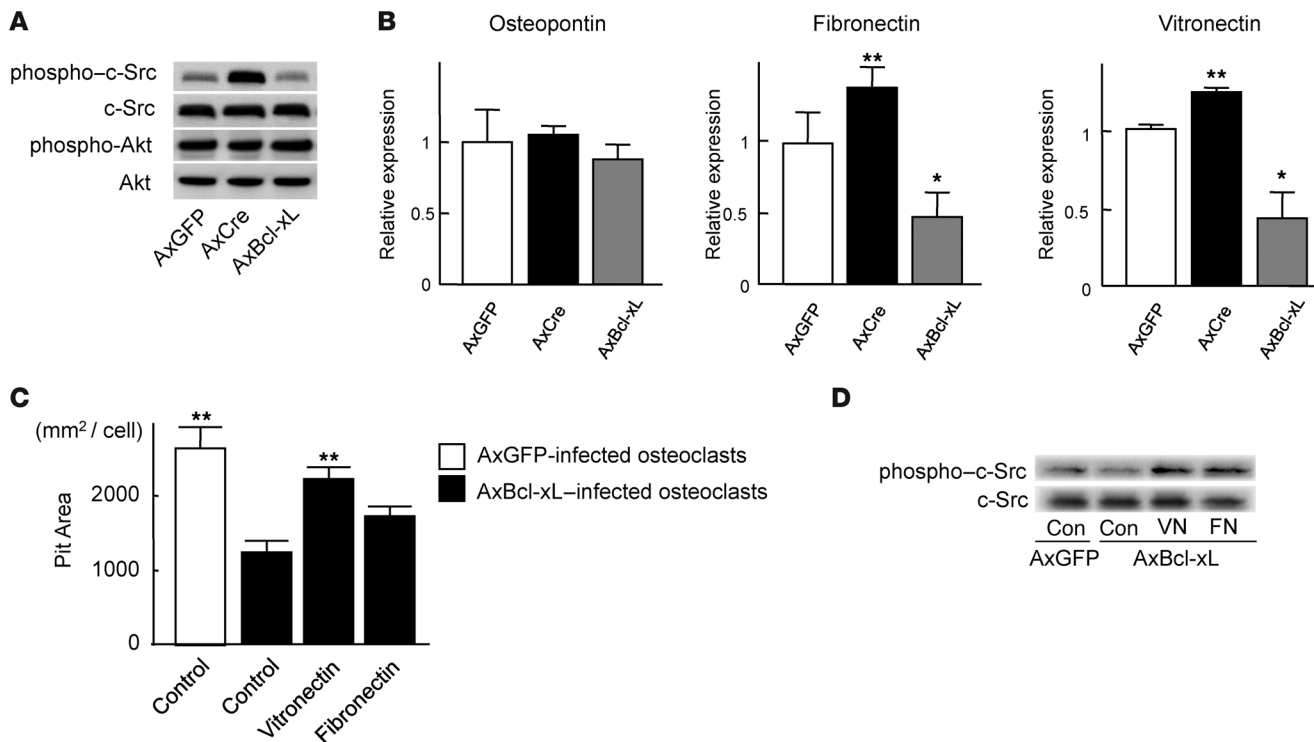


Figure 7

Bcl-xL reduced c-Src activity in osteoclasts by suppressing the expression of ECM proteins. (A) Western blotting with anti-phospho-c-Src antibody and anti-phospho-Akt antibody. Osteoclasts generated from *Bcl-x^{fl/fl}* mouse bone marrow cells were infected with AxBcl-xL. After 24 h of infection, the lysates were subjected to Western blotting. c-Src was activated in *Bcl-x* cKO osteoclasts, while no difference in Akt activation was observed. The amount of total c-Src or Akt did not appear to differ. (B) mRNA expression of osteopontin, vitronectin, and fibronectin by real-time RT-PCR. Vitronectin and fibronectin expression increased in *Bcl-x* cKO osteoclasts and decreased in Bcl-xL-overexpressing osteoclasts. Results are mean ± SD of 6 samples. **P* < 0.01, ***P* < 0.05 versus AxBcl-xL-infected cells. (C) Effect of ECM protein coating on bone-resorbing activity of AxBcl-xL-infected osteoclasts. When AxBcl-xL-infected osteoclasts were cultured on vitronectin- or fibronectin-coated dentine slices, the negative effect of Bcl-xL overexpression on bone resorption was partially reversed, and vitronectin-coated dentine slices showed a significant increase in pit area. Results are mean ± SD of 4 cultures. ***P* < 0.05 versus AxBcl-xL-infected osteoclasts cultured on uncoated control dentine slices. (D) Western blotting with anti-phospho-c-Src antibody and anti-Src antibody. c-Src activity suppressed by AxBcl-xL expression in osteoclasts was partially restored by plating the cells onto vitronectin- or fibronectin-coated dishes. The total amount of c-Src did not appear to differ.

Discussion

Here we have demonstrated what we believe to be a novel function of the antiapoptotic molecule Bcl-xL to modulate bone-resorbing activity of osteoclasts by regulating ECM protein production and c-Src kinase activity. Previous studies have suggested a possible role of Bcl-xL in the survival of osteoclasts. Pioneering work by Roodman and coworkers demonstrated that the targeting of Bcl-xL and SV40 large T antigen to cells of the osteoclast lineage in transgenic mice under the control of the TRAP promoter immortalized osteoclast precursors (19). Zhang et al. reported that TNF-α inhibited alendronate-induced apoptosis of osteoclasts by stimulating Bcl-xL expression (20). On the other hand, Jimi et al. (21) reported that Bcl-2 and Bcl-xL in osteoclasts were not upregulated by RANKL treatment. In the present study, we found that 10 μM ABT-737 severely diminished osteoclast survival (Figure 1A). Unexpectedly, ABT-737 treatment upregulated the bone-resorbing activity of osteoclasts (Figure 1B), which suggests that antiapoptotic Bcl-2 family proteins positively regulate osteoclast survival and negatively regulate osteoclast activity, although it is possible that the inhibitor treatment specifically selected the relatively active osteoclasts.

To further elucidate the physiological role of Bcl-xL in osteoclasts, we generated *Bcl-x* cKO mice. We found that the mice exhibited osteopenia as a result of increased bone-resorbing activity of osteoclasts. Osteoclasts generated from *Bcl-x* cKO mouse bone marrow cells exhibited reduced survival and increased bone-resorbing activity, consistent with the results obtained in the inhibitor experiments.

We previously reported that activation of the Erk pathway through the introduction of constitutively active Mek1 markedly promoted the survival of osteoclasts, and that, conversely, inhibition of the pathway by overexpressing Ras^{DN} rapidly induced apoptotic cell death (14). The exact mechanisms by which the Erk pathways regulates osteoclast survival have not been clarified yet, but we previously found that the proapoptotic Bcl-2 family protein Bim induces apoptosis of osteoclasts and that the Erk pathways negatively regulate Bim expression through the ubiquitin-proteasome degradation system (22). In the present study, we established that the expression of Bcl-xL in osteoclasts was induced upon activation of the Erk pathway by Mek^{CA} and was decreased through suppression by Ras^{DN}. Overexpression of Bcl-xL almost completely



compensated for the apoptotic effect of Ras^{DN} or PD98059, while Erk activation by Mek^{CA} expression only partially restored the survival of *Bcl-x*-deleted osteoclasts. These results suggest that Bcl-xL lies downstream of Erk in the signaling cascade and that the balance between Bcl-xL and Bim critically regulates osteoclast survival. Overexpression of Bcl-xL suppressed, and *Bcl-x* knockout increased, Erk activity in osteoclasts, suggestive of negative feedback regulation of Erk activity by Bcl-xL.

In spite of the proapoptotic tendency of *Bcl-x* cKO osteoclasts, these cells exhibited increased bone-resorbing activity. This is in sharp contrast to the phenotype observed in *Bim* KO osteoclasts, which exhibited decreased bone-resorbing activity along with increased apoptosis (22). In an attempt to identify the molecular mechanisms underlying the increased bone-resorbing function of osteoclasts, we identified that Bcl-xL regulated integrin-mediated c-Src activation in osteoclasts through modulating ECM protein expression. Integrins are transmembrane heterodimeric glycoproteins consisting of α and β subunits that mediate cell-cell and cell-matrix interactions (23). Ligand binding to integrins activates intracellular signal transduction pathways, which lead to de novo gene expression and the cytoskeletal rearrangement associated with cell adhesion, spreading, and migration (24, 25). The $\alpha_v\beta_3$ integrin, also known as the vitronectin receptor, is predominantly expressed in osteoclasts (26). Sanjay et al. (27) previously reported that the engagement of $\alpha_v\beta_3$ integrin induces the formation of a Pyk2/c-Src/c-Cbl complex, resulting in c-Src activation and osteoclastic bone resorption, and that *c-Src* KO osteoclasts exhibit decreased motility on vitronectin-coated surfaces in vitro. We found that Bcl-xL had a negative effect on c-Src kinase activity and vitronectin and fibronectin mRNA levels in osteoclasts (Figure 7, A and B). In addition, suppression of bone-resorbing activity of osteoclasts by Bcl-xL overexpression was partially restored by coating the dentine slices with fibronectin or vitronectin (Figure 7C). These results suggest that Bcl-xL-regulated ECM protein production plays an important role in the bone-resorbing activity of osteoclasts, modulating integrin function and c-Src activity in an autocrine/paracrine fashion. Recently, a critical link between Bcl-xL and tumor cell invasion was reported (28, 29), which may also be caused by the modulation of ECM protein production by Bcl-xL. Li et al. reported that inositol 1,4,5-triphosphate receptors (IP₃Rs), intracellular Ca²⁺ channels gated by the secondary messenger IP₃ (30), was significantly downregulated by Bcl-xL expression. In addition, expression of Bcl-xL decreased the induction of NFAT DNA binding to the IP₃R promoter and the transcription of IP₃R (31, 32), which may lead to the downregulation of ECM protein production. The role of IP₃ signaling on ECM expression in osteoclasts remains elusive, and future studies are required.

Interestingly, although *Bcl-x* deficiency reduced the survival of osteoclasts in vitro, the number of osteoclasts in *Bcl-x* cKO mice was equivalent to that in normal littermates. The exact reason for this discrepancy remains elusive, but it is possible that the apoptosis of the cells is recovered by the presence of supporting cells, such as osteoblasts, and of the cytokines they produce, such as M-CSF; alternatively, other antiapoptotic Bcl-2 family members may substitute the antiapoptotic function of Bcl-xL in vivo. It is also possible that *Bcl-x* deficiency instead increased the differentiation of the osteoclasts. Further studies are required to clarify the role of Bcl-xL in osteoclast differentiation.

In conclusion, the results of the present study demonstrate that Bcl-xL plays a pivotal role not only in apoptosis of osteoclasts, but

also in bone-resorbing function of the cells. Further investigation of these pathways in osteoclasts will give new insights into the molecular mechanisms regulating osteoclast function.

Methods

Animals. *Bcl-x*^{fl/fl} mice, carrying the *Bcl-x* gene with 2 loxP sequences in the promoter region and the second intron, were generated as previously described (33). The mice are on a 129SvEv and C57BL/6 mixed background. The presence of the floxed *Bcl-x* gene was determined by PCR around the 5' loxP site using the primers 5'-CGGTTGCCTAGCAACGGGGC-3' and 5'-CTCCCACAGTGGAGACCTCG-3', giving a wild-type band of 200 bp and a floxed gene product of 300 bp. *Bcl-x*^{fl/fl} mice have previously been used successfully to examine the role of Bcl-xL in a variety of cell types, including those in the liver, ovary, mammary gland, and substantia nigra, as well as in erythroid cells and dendritic cells (33–38). To generate *Bcl-x* cKO mice, we used cathepsin K-Cre mice, in which the Cre recombinase gene is knocked into the *cathepsin K* locus and specifically expressed in osteoclasts (13). *Bcl-x* cKO mice and normal *Bcl-x*^{fl/fl} littermates were generated by mating Cathepsin K-Cre^{+/+}*Bcl-x*^{fl/+} male mice with Cathepsin K-Cre^{-/-}*Bcl-x*^{fl/fl} female mice. All animals were housed under specific pathogen-free conditions and treated with humane care under approval from the Animal Care and Use Committee of the University of Tokyo.

Serum CTx-I measurement. Blood samples were collected retro-orbitally under anesthesia immediately prior to sacrifice. Serum CTx-I, a specific marker of osteoclastic bone resorption, was measured using a RatLaps ELISA kit (Nordic Bioscience Diagnostics A/S). Plasma was obtained using plasma separator tubes with lithium heparin (Becton Dickinson).

Histological analyses. Tissues were fixed in 4% paraformaldehyde/PBS, decalcified in 10% EDTA, embedded in paraffin, and cut into sections of 4- μ m thickness. H&E staining was performed according to the standard procedure. Histomorphometric analysis was performed in undecalcified sections from 0.15 mm below the growth plate to 0.6 mm of the primary spongiosa of the proximal tibia. For double labeling, mice were injected subcutaneously with 16 mg/kg body weight of calcein on days 6 and 1 before sacrifice.

Generation of osteoclasts and survival/bone resorption assay. Bone marrow cells were obtained from the femur and tibia of male ddY or *Bcl-x*^{fl/fl} mice at 5 weeks of age, and bone marrow macrophages were cultured in α -MEM (Gibco; Invitrogen) containing 10% FBS (Sigma-Aldrich) in the presence of 100 ng/ml M-CSF (R&D Systems) for 2 days. Osteoclasts were generated by stimulating bone marrow macrophages with 10 ng/ml M-CSF and 100 ng/ml RANKL (Wako Pure Chemical) for an additional 4–5 days or by the coculture system established by Takahashi (39).

Survival assay was performed as follows. After osteoclasts were generated, both RANKL and M-CSF were removed from the culture (time 0), and osteoclasts were cultured for the indicated times. The Bcl-2/Bcl-xL inhibitor ABT-737, a small-molecule BH3 mimetic that binds to and antagonizes Bcl-2 and Bcl-xL, was provided by Abbott Laboratories. The survival rate of the cells was estimated as the percentage of morphologically intact TRAP⁺ multinucleated cells compared with those at time 0.

Bone resorption assay of osteoclasts was performed as previously reported (14). Briefly, osteoclasts were generated by cocultures of osteoblasts and bone marrow cells on collagen gel-coated dishes in the presence of 10 nM 1 α ,25(OH)₂vitamin D₃ and 1 μ M PGE₂. On day 6 of culture, when osteoclasts were differentiated, the cells were dispersed by treating with 0.1% bacterial collagenase (Wako Pure Chemical) for 10 minutes. The cells were resuspended in α -MEM containing 10% FBS, replated on dentine slices, and cultured for the indicated times. After cells were removed by treating the dentine slices with 1 M NH₄OH, the resorption areas were visualized by staining with 1% toluidine blue. Resorption pit area was quantified using an image analysis system (MICROANALYZER).



Expression constructs and gene transduction. Adenoviruses carrying the Cre recombinase gene (provided by K. Ueki, University of Tokyo) were amplified in HEK293 cells and purified with the AdenoX Virus Purification Kit (Clontech). Viral titers were determined by the end point dilution assay, and the viruses were used at 50 MOI. Adenoviral infection of osteoclasts was performed as previously reported (40, 41). In short, on day 4 of culture, when osteoclasts began to appear, mouse cocultures were incubated for 1 hour at 37°C with a small amount of α -MEM containing the recombinant adenoviruses at the desired MOI. Cells were then washed twice with PBS and further incubated at 37°C in α -MEM containing 10% FBS, 10 nM $1\alpha,25(\text{OH})_2\text{D}_3$, and 1 μM PGE₂. Experiments were performed 2 days after the infection. Adenovirus vectors used in the experiments, and the genes carried by the vectors, are as follows: AxGFP (green fluorescence protein gene), AxBcl-xL (*bcl-xL* gene), AxCre (Cre recombinase gene), AxMek^{CA} (constitutively active *mek1* gene), AxRas^{DN} (dominant-negative *ras* gene).

Real-time PCR. Total RNA was extracted with ISOGEN (Wako Pure Chemical), and an aliquot (1 μg) was reverse-transcribed using a QuantiTect Reverse Transcription Kit (QIAGEN) to make single-stranded cDNA. PCR was performed on an ABI Prism 7000 Sequence Detection System (Applied Biosystems) using QuantiTect SYBR Green PCR Master Mix (QIAGEN) according to the manufacturer's instructions. All reactions were run in triplicate. After data collection, the mRNA copy number of a specific gene in the total RNA was calculated with a standard curve generated with serially diluted plasmids containing PCR amplicon sequences, and normalized to the rodent total RNA with mouse β -actin as an internal control. Standard plasmids were synthesized with a TOPO TA Cloning Kit, according to the manufacturer's instruction. Primer sequences for endogenous genes were as follows: Bcl-xL, 5'-GCTGGGACACTTTTGTGGAT-3' and 5'-TGTCTGGTCACTTCCGACTG-3'; β -actin, 5'-AGATGTGGAT-CAGCAAGCAG-3' and 5'-GCGCAAGTTAGGTTTTGTCA-3'; osteopontin, 5'-ACATTTCACTCCAATCGTCC-3' and 5'-TGCCCTTCCGTTGTTGTCC-3'; vitronectin, 5'-GGAGCCCAAGAACAATACCA-3' and 5'-TCTCCTCTGTTGCTCCACT-3'; fibronectin, 5'-CAGCAGTATGGC-CACAGAGA-3' and 5'-AAAGCTGCTGGCTGTGATTT-3'.

Western blotting. Cells were washed with ice-cold PBS, and proteins were extracted with Tris-HCl, NaCl, and EDTA (TNE) buffer (1% NP-40; 10 mM Tris-HCl, pH 7.8; 150 mM NaCl; 1 mM EDTA; 2 mM Na₃VO₄; 10 mM NaF;

and 10 g/ml aprotinin). For Western blotting analysis, lysates were fractionated by SDS-PAGE with 7.5%–15% Tris-Glycin gradient gel or 15% Tris-Glycin gel and transferred onto nitrocellulose membranes (BIO-RAD). After blocking with 6% milk/TBS-T, membranes were incubated with primary antibodies to Bcl-xL, cleaved caspase-3, phospho-c-Src (Cell Signaling Technology), Src (Santa Cruz Biotechnology Inc.), or β -actin (Sigma-Aldrich) followed by HRP-conjugated goat anti-mouse IgG and goat anti-rabbit IgG (Promega). Immunoreactive bands were visualized with ECL Plus (Amersham) according to the manufacturer's instructions. The blots were stripped by incubating for 20 minutes in stripping buffer (2% SDS; 100 mM 2-mercaptoethanol; and 62.5 mM Tris-HCl, pH 6.7) at 50°C and reprobed with the other antibodies.

Statistics. Statistical analyses were performed using a 2-tailed unpaired Student's *t* test (Figures 1–4) or ANOVA analysis (Figures 5–7), and each series of experiments was repeated at least 3 times. Results are presented as mean \pm SD.

Acknowledgments

The authors thank R. Yamaguchi (Department of Orthopaedic Surgery, University of Tokyo) for providing expert technical assistance. ABT-737 was provided by Abbott Laboratories. This work was supported in part by Grants-in-Aid from the Ministry of Education, Culture, Sports, Science, and Technology of Japan and by Health Science research grants from the Ministry of Health, Labor, and Welfare of Japan to S. Tanaka. The research of L. Hennighausen was funded through the Intramural Program of the National Institute of Diabetes and Digestive and Kidney Diseases, NIH. Pacific Edit reviewed the manuscript prior to submission.

Received for publication May 11, 2009, and accepted in revised form July 22, 2009.

Address correspondence to: Sakae Tanaka, Department of Orthopaedic Surgery, Faculty of Medicine, University of Tokyo, 7-3-1 Hongo, Bunkyo-ku, Tokyo 113-0033, Japan. Phone: 81-3-3815-5411 ext. 33376; Fax: 81-3-3818-4082; E-mail: TANAKAS-ORT@h.u-tokyo.ac.jp.

1. Suda, T., Nakamura, I., Jimi, E., and Takahashi, N. 1997. Regulation of osteoclast function. *J. Bone Miner. Res.* **12**:869–879.
2. Roodman, G.D. 1999. Cell biology of the osteoclast. *Exp. Hematol.* **27**:1229–1241.
3. Lakkakorpi, P., Tuukkanen, J., Hentunen, T., Jarvelin, K., and Vaananen, K. 1989. Organization of osteoclast microfilaments during the attachment to bone surface in vitro. *J. Bone Miner. Res.* **4**:817–825.
4. Lakkakorpi, P.T., and Vaananen, H.K. 1991. Kinetics of the osteoclast cytoskeleton during the resorption cycle in vitro. *J. Bone Miner. Res.* **6**:817–826.
5. Kim, H., et al. 2006. Hierarchical regulation of mitochondrion-dependent apoptosis by BCL-2 subfamilies. *Nat. Cell Biol.* **8**:1348–1358.
6. White, E. 1996. Life, death, and the pursuit of apoptosis. *Genes Dev.* **10**:1–15.
7. Yang, E., and Korsmeyer, S.J. 1996. Molecular thanatopsis: a discourse on the BCL2 family and cell death. *Blood.* **88**:386–401.
8. Lithgow, T., van Driel, R., Bertram, J.F., and Strasser, A. 1994. The protein product of the oncogene *bcl-2* is a component of the nuclear envelope, the endoplasmic reticulum, and the outer mitochondrial membrane. *Cell Growth Differ.* **5**:411–417.
9. Krajewski, S., et al. 1993. Investigation of the subcellular distribution of the *bcl-2* oncogene: residence in the nuclear envelope, endoplasmic reticulum, and outer mitochondrial membranes. *Cancer Res.* **53**:4701–4714.
10. Boise, L.H., et al. 1993. *bcl-x*, a *bcl-2*-related gene that functions as a dominant regulator of apoptotic cell death. *Cell.* **74**:597–608.
11. Motoyama, N., et al. 1995. Massive cell death of immature hematopoietic cells and neurons in *Bcl-x* deficient mice. *Science.* **267**:1506–1510.
12. Oltersdorf, T., et al. 2005. An inhibitor of *Bcl-2* family proteins induces regression of solid tumours. *Nature.* **435**:677–681.
13. Nakamura, T., et al. 2007. Estrogen prevents bone loss via estrogen receptor alpha and induction of Fas ligand in osteoclasts. *Cell.* **130**:811–823.
14. Miyazaki, T., et al. 2000. Reciprocal role of ERK and NF-kappaB pathways in survival and activation of osteoclasts. *J. Cell Biol.* **148**:333–342.
15. Soriano, P., Montgomery, C., Geske, R., and Bradley, A. 1991. Targeted disruption of the *c-src* proto-oncogene leads to osteopetrosis in mice. *Cell.* **64**:693–702.
16. Tanaka, S., et al. 1996. *c-Cbl* is downstream of *c-Src* in a signalling pathway necessary for bone resorption. *Nature.* **383**:528–531.
17. Longhurst, C.M., and Jennings, L.K. 1998. Integrin-mediated signal transduction. *Cell. Mol. Life Sci.* **54**:514–526.
18. Duong, L.T., and Rodan, G.A. 1998. Integrin-mediated signaling in the regulation of osteoclast adhesion and activation. *Front. Biosci.* **3**:d757–d768.
19. Hentunen, T.A., et al. 1998. Immortalization of osteoclast precursors by targeting *Bcl-XL* and Simian virus 40 large T antigen to the osteoclast lineage in transgenic mice. *J. Clin. Invest.* **102**:88–97.
20. Zhang, Q., et al. 2005. Tumor necrosis factor prevents alendronate-induced osteoclast apoptosis in vivo by stimulating *Bcl-xL* expression through *Ets-2*. *Arthritis Rheum.* **52**:2708–2718.
21. Jimi, E., et al. 1999. Osteoclast differentiation factor acts as a multifunctional regulator in murine osteoclast differentiation and function. *J. Immunol.* **163**:434–442.
22. Akiyama, T., et al. 2003. Regulation of osteoclast apoptosis by ubiquitylation of proapoptotic BH3-only *Bcl-2* family member *Bim*. *EMBO J.* **22**:6653–6664.
23. Hynes, R.O. 1987. Integrins: a family of cell surface receptors. *Cell.* **48**:549–554.
24. Thomas, S.M., and Brugge, J.S. 1997. Cellular functions regulated by Src family kinases. *Annu. Rev. Cell Dev. Biol.* **13**:513–609.
25. Giancotti, F.G., and Ruoslahti, E. 1999. Integrin signaling. *Science.* **285**:1028–1032.
26. Davies, J., et al. 1989. The osteoclast functional antigen, implicated in the regulation of bone resorption, is biochemically related to the vitronectin receptor. *J. Cell Biol.* **109**:1817–1826.
27. Sanjay, A., et al. 2001. *Cbl* associates with *Pyk2* and



- Src to regulate Src kinase activity, alpha(v)beta(3) integrin-mediated signaling, cell adhesion, and osteoclast motility. *J. Cell Biol.* **152**:181–195.
28. Du, Y.C., Lewis, B.C., Hanahan, D., and Varmus, H. 2007. Assessing tumor progression factors by somatic gene transfer into a mouse model: Bcl-xL promotes islet tumor cell invasion. *PLoS Biol.* **5**:e276.
29. Martin, S.S., et al. 2004. A cytoskeleton-based functional genetic screen identifies Bcl-xL as an enhancer of metastasis, but not primary tumor growth. *Oncogene.* **23**:4641–4645.
30. Li, C., et al. 2002. Bcl-X(L) affects Ca(2+) homeostasis by altering expression of inositol 1,4,5-trisphosphate receptors. *Proc. Natl. Acad. Sci. U. S. A.* **99**:9830–9835.
31. Genazzani, A.A., Carafoli, E., and Guerini, D. 1999. Calcineurin controls inositol 1,4,5-trisphosphate type 1 receptor expression in neurons. *Proc. Natl. Acad. Sci. U. S. A.* **96**:5797–5801.
32. Graef, I.A., et al. 1999. L-type calcium channels and GSK-3 regulate the activity of NF-ATc4 in hippocampal neurons. *Nature.* **401**:703–708.
33. Rucker, E.B., 3rd, et al. 2000. Bcl-x and Bax regulate mouse primordial germ cell survival and apoptosis during embryogenesis. *Mol. Endocrinol.* **14**:1038–1052.
34. Hon, H., Rucker, E.B., 3rd, Hennighausen, L., and Jacob, J. 2004. bcl-xL is critical for dendritic cell survival in vivo. *J. Immunol.* **173**:4425–4432.
35. Riedlinger, G., et al. 2002. Bcl-x is not required for maintenance of follicles and corpus luteum in the postnatal mouse ovary. *Biol. Reprod.* **66**:438–444.
36. Savitt, J.M., Jang, S.S., Mu, W., Dawson, V.L., and Dawson, T.M. 2005. Bcl-x is required for proper development of the mouse substantia nigra. *J. Neurosci.* **25**:6721–6728.
37. Wagner, K.U., et al. 2000. Conditional deletion of the Bcl-x gene from erythroid cells results in hemolytic anemia and profound splenomegaly. *Development.* **127**:4949–4958.
38. Walton, K.D., et al. 2001. Conditional deletion of the bcl-x gene from mouse mammary epithelium results in accelerated apoptosis during involution but does not compromise cell function during lactation. *Mech. Dev.* **109**:281–293.
39. Takahashi, N., et al. 1988. Osteoblastic cells are involved in osteoclast formation. *Endocrinology.* **123**:2600–2602.
40. Tanaka, S., et al. 1998. Modulation of osteoclast function by adenovirus vector-induced epidermal growth factor receptor. *J. Bone Miner. Res.* **13**:1714–1720.
41. Miyazaki, T., Neff, L., Tanaka, S., Horne, W.C., and Baron, R. 2003. Regulation of cytochrome c oxidase activity by c-Src in osteoclasts. *J. Cell Biol.* **160**:709–718.